An iterated multiplicative regularization for force reconstruction problems

Mathieu Aucejo, Olivier de Smet

An iterated multiplicative regularization for force reconstruction problems

M. Aucejo[a], O. De Smet[a]

[a]*Structural Mechanics and Coupled Systems Laboratory, Conservatoire National des Arts et Métiers, 2 Rue Conté, 75003 Paris, France*

Abstract

In presence of very noisy data, standard regularization methods generally fail in reconstructing satisfying solutions. To this end, iterated regularization techniques can be implemented. This class of regularization approaches can be seen as an iterative refinement of an initial solution obtained from classical regularization methods. In the present paper, an iterated multiplicative regularization for dealing with force reconstruction problems is discussed. More specifically, the associated non-stationary formulation is compared to its stationary counterpart through numerical and experimental validations. It is shown that the proposed stationary version outperforms the non-stationary formulation regarding the quality of reconstructed solutions.

Keywords: Inverse problem, Force reconstruction, Multiplicative regularization, Iterated regularization.

1. Introduction

Iterated Tikhonov regularization has been extensively studied by the inverse problem community. Classically, iterated Tikhonov regularization is

*Corresponding author. E-mail address: mathieu.aucejo@cnam.fr

defined as follows:

$$\begin{cases} \widehat{\mathbf{F}}^{(0)} = \mathbf{0} \\ \widehat{\mathbf{F}}^{(k)} = \underset{\mathbf{F}}{\operatorname{argmin}} \ \|\mathbf{X} - \mathbf{H}\mathbf{F}\|_2^2 + \lambda^{(k)} \left\|\mathbf{F} - \widehat{\mathbf{F}}^{(k-1)}\right\|_2^2 \quad \text{for } k \geq 1 \end{cases}, \tag{1}$$

where in the context of force reconstruction $\mathbf{X}$ is the measured vibration field, $\mathbf{H}$ is the system matrix of the structure describing its dynamic behavior, $\widehat{\mathbf{F}}^{(k)}$ is the force vector identified at iteration k and $\lambda^{(k)}$ is the regularization parameter at iteration k.

The previous formulation is referred to as non-stationary Tikhonov regularization [1, 2, 3, 4, 5, 6], because the regularization parameter changes at each iteration. If the regularization parameter remains constant over the iterations, it is called stationary iterated Tikhonov regularization [5, 6, 7, 8, 9, 10, 11]. Practically, iterated Tikhonov regularization can be viewed as an iterative refinement of an initial solution obtained by applying the standard Tikhonov regularization [12]. Surprisingly, this regularization strategy seems to be seldom applied in mechanics despite its ability to compute improved identified solutions [13, 14].

In the context of force identification, iterated Tikhonov regularization has two major drawbacks. First, the regularization term promotes distributed solutions, which is not desirable when the structure is actually excited by localized or impulsive sources. This problem can be solved by implementing the iterated Tikhonov regularization in Banach spaces instead of Hilbert spaces [15, 16, 17]. Practically, this means that the regularization term is express as the ℓ_q-norm of the residual solution $\mathbf{F} - \widehat{\mathbf{F}}^{(k-1)}$. Such a regulariza-

tion term is highly flexible to express one's prior knowledge on the sources to identify, since smooth solutions are promoted for $q = 2$ [18, 19], while sparse excitation fields are obtained with $q \leq 1$ [20, 21, 22, 23, 24, 25, 26, 27, 28, 29]. The second limiting factor is the estimation of the regularization parameter λ, that can be computed through automatic selection procedures such as the L-curve principle [30] or the Generalized Cross-Validation [31]. Indeed, when the reconstruction problem becomes large, this calculation can be very expensive, because they are usually based on the computation the Singular Value Decomposition (SVD) of the system matrix $\mathbf{H}$. In this respect, the multiplicative regularization [32, 33, 34, 35] is an interesting alternative, since it eliminates the need for the selection of the optimal regularization. However, as shown in the next of the paper, when this strategy is applied to very noisy data, as any Tikhonov-like regularization, identified solutions are generally disappointing. In such a situation an iterated approach is particularly well suited.

To combine the best of both worlds, an original iterated multiplicative regularization is proposed. In this paper, the main features of the proposed regularization strategy are set out, while its validity is assessed through a series numerical and real-world experiments. To clearly introduce the main features of the proposed strategy, this contribution is divided into four parts. Before considering the core of the paper, the need for another regularization strategy is explained in section 2. Section 3 is devoted to the introduction of the proposed iterated multiplicative regularization. More precisely, a non-stationary version is introduced as well as its stationary counterpart. The

comparison of both formulations is performed numerically in section 4 on two frequency domain applications. Obtained results demonstrate perhaps counterintuitively that proposed stationary formulation outperforms the associated non-stationary version regarding the quality of reconstructed solutions. The experimental validation presented in section 5 allows confirming the conclusions drawn in the numerical validation.

2. The need for another regularization strategy

As mentioned in the introduction, the iterated Tikhonov regularization given by Eq. (1) can lead to inaccurate reconstructions when the excitation field to identify is sparse. To illustrate this, let us consider the reconstruction in the frequency domain of a harmonic unit point force exciting a free-free steel beam at 350 Hz from a noisy measured vibration displacement field having a certain signal-to-noise ratio (SNR) [see section 4.1 for a detailed description of the test case].

Let us first consider the situation where the SNR is relatively high, e.g. 30 dB. In this case, it is clear from Fig. 1 that neither the standard Tikhonov regularization nor its stationary iterated version using the regularization parameter computed at the first iteration, namely $\lambda^{(1)}$, from the L-curve principle give a satisfying identified solution. Indeed, the analysis of the result shows that the reconstructed excitation fields are too smooth compared to the target one. It should also be noted that the non-stationary iterated Tikhonov regularization does not provide a better identified solution. Indeed, for a

traditional choice of $\lambda^{(k)}$, namely [36]:

$$\lambda^{(k)} = \lambda^{(1)}\beta^{k-1}, \quad \text{with} \quad \beta \in [0, 1], \tag{2}$$

$\lambda^{(k)}$ decreases as k increases. As a result, if the regularization parameter $\lambda^{(1)}$ is optimally selected from the L-curve principle for instance, then the non-stationary iterated Tikhonov regularization leads to the least squares solution.

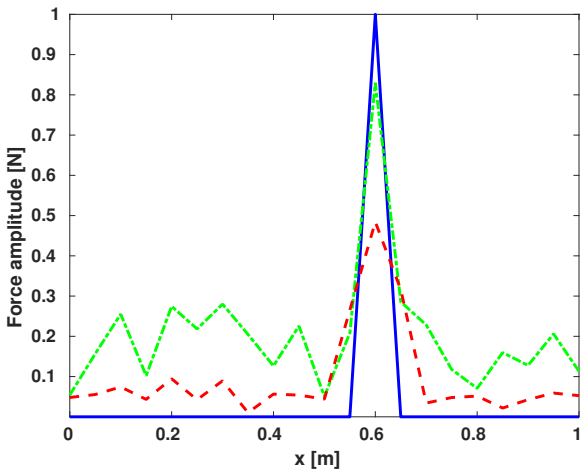

Figure 1: Reconstruction of the excitation field at 350 Hz from a measured vibration field with high SNR (30 dB) - (—) Reference, (– –) Standard Tikhonov regularization and (– · –) Stationary iterated Tikhonov regularization.

As explained in the introduction, the previous formulation has two drawbacks, since it does not exploit one's prior knowledge of the sources to identify and it requires the calculation of a regularization parameter, which can be computationally intensive depending on the size of the reconstruction problem. To bypass these potential difficulties, a multiplicative regularization has been introduced [34, 35]. Formally, it consists in solving the following

minimization problem:

$$\widehat{\mathbf{F}} = \underset{\mathbf{F}\setminus\{\mathbf{0}\}}{\operatorname{argmin}} \, \|\mathbf{X} - \mathbf{H}\mathbf{F}\|_2^2 \cdot \|\mathbf{F}\|_q^q \,, \tag{3}$$

where q is the norm parameter included in the interval $]0, +\infty[$, $\| \bullet \|_q$ is the ℓ_q-norm or quasi-norm. Practically, q is set to 2 if the solution is supposed to be distributed, while q can be chosen equal to or less than 1 if the solution is supposed to be localized [26].

The application of the multiplicative regularization from the measured vibration field used previously gives, when $q = 0.5$, the reconstruction field presented in Figure 2. This figure shows that the reference excitation field and the reconstructed one are very close together when the measured data are little noisy (high SNR). Unfortunately, when the data are very noisy (low SNR), a degradation of the regularized solution accuracy is observed [see Figure 2].

In the light of these observations, it seems interesting to develop an iterated multiplicative regularization, combining the benefits of the multiplicative regularization and the iterated Tikhonov regularization. In particular, such an approach is potentially able to provide a refined regularized solution, while exploiting prior information on the sources to identify.

3. Iterated multiplicative regularization

This section aims at introducing the non-stationary iterated multiplicative regularization as well as its stationary counterpart. To render the pre-

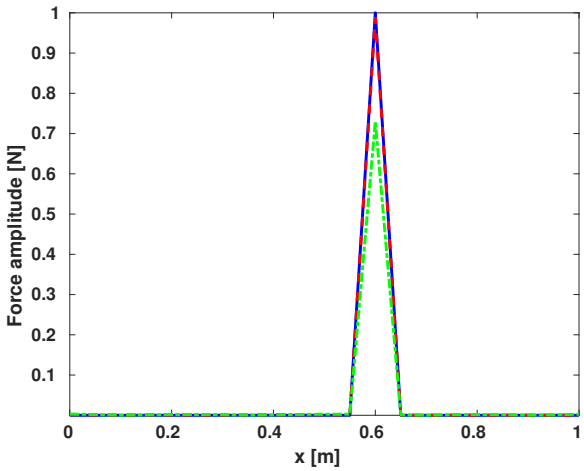

Figure 2: Reconstruction of the excitation field at 350 Hz from a measured vibration field - (—) Reference, (– –) Multiplicative regularization for $q = 0.5$ and SNR = 30 dB and (– · –) Multiplicative regularization for $q = 0.5$ and SNR = 13 dB.

sentation more didactic, it is focused on the main concepts and features of the method.

3.1. Non-stationary version

By analogy with the standard iterated Tikhonov regularization, the non-stationary iterated multiplicative regularization (NSIMR) is expressed as:

$$\begin{cases} \widehat{\mathbf{F}}^{(0)} = \mathbf{0} \\ \widehat{\mathbf{F}}^{(k)} = \underset{\mathbf{F} \setminus \left\{\widehat{\mathbf{F}}^{(k-1)}\right\}}{\operatorname{argmin}} \|\mathbf{X} - \mathbf{H}\mathbf{F}\|_2^2 \cdot \left\|\mathbf{F} - \widehat{\mathbf{F}}^{(k-1)}\right\|_q^q \quad \text{for } k \geq 1 \end{cases} . \tag{4}$$

Practically, the resolution of the minimization problem at iteration $k \geq 1$ requires the implementation of an iterative procedure. In the present contribution, an Iteratively Reweighted Least Squares (IRLS) algorithm is implemented. Basically, it consists in iteratively computing the solution of the

problem by recasting the ℓ_q-norm into a weighted ℓ_2-norm. As a result, at iteration k of the proposed iterated regularization, the estimated force vector $\widehat{\mathbf{F}}^{(k,j)}$ at iteration j of the IRLS algorithm is explicitly given by [34]:

$$\widehat{\mathbf{F}}^{(k,j)} = \left[\mathbf{H}^H\mathbf{H} + \alpha^{(k,j)}\mathbf{W}^{(k,j-1)}\right]^{-1}\left[\mathbf{H}^H\mathbf{X} + \alpha^{(k,j)}\mathbf{W}^{(k,j-1)}\widehat{\mathbf{F}}^{(k-1)}\right], \quad (5)$$

where:

- $\mathbf{W}^{(k,j-1)}$ is a diagonal weighting matrix depending on the norm parameter q and the residual solution at iteration $j-1$, namely $\mathbf{R}^{(k,j-1)} = \widehat{\mathbf{F}}^{(k,j-1)} - \widehat{\mathbf{F}}^{(k-1)}$ [25, 34, 26, 37]. For the sake of completeness, it should be mentioned that the i$^{\text{th}}$ component of the weighting matrix at iterations outer iteration k and inner iteration $j-1$, $w_i^{(k,j-1)}$, is expressed as:

$$w_i^{(k,j-1)} = \max\left(\epsilon^{(k)}, \left|r_i^{(k,j-1)}\right|\right)^{q-2}, \quad (6)$$

  where $r_i^{(k,j-1)}$ is the i$^{\text{th}}$ of the residual solution $\mathbf{R}^{(k,j-1)}$ and $\epsilon^{(k)}$ is a small real positive number acting as a damping parameter. It allows avoiding infinite weights when $\left|r_i^{(k,j-1)}\right| \to 0$ and $q < 2$. Its value is selected at the beginning of each outer iteration so that 5% of the values of $\left|\mathbf{R}^{(k,0)}\right|$ are less than or equal to $\epsilon^{(k)}$.

- $\alpha^{(k,j)}$ is the adaptive regularization parameter[1], defined such that:

$$\alpha^{(k,j)} := \frac{\left\|\mathbf{X} - \mathbf{H}\widehat{\mathbf{F}}^{(k,j-1)}\right\|_2^2}{\left\|\mathbf{W}^{(k,j-1)^{1/2}}\left(\widehat{\mathbf{F}}^{(k,j-1)} - \widehat{\mathbf{F}}^{(k-1)}\right)\right\|_2^2}. \quad (7)$$

[1] because its value is updated at each iteration of the IRLS algorithm.

When the IRLS algorithm has converged after N_j iterations, the solution vector $\widehat{\mathbf{F}}^{(k)}$, the weighting matrix $\mathbf{W}^{(k)}$ and the adaptive regularization parameter $\alpha^{(k)}$ are returned by the algorithm and are defined such that:

$$\widehat{\mathbf{F}}^{(k)} := \widehat{\mathbf{F}}^{(k,N_j)}, \quad \mathbf{W}^{(k)} := \mathbf{W}^{(k,N_j)} \quad \text{and} \quad \alpha^{(k)} := \alpha^{(k,N_j)}. \tag{8}$$

Consequently, the previous non-stationary iterated multiplicative algorithm is composed of a main (outer) iteration corresponding to the refinement stage and a nested (inner) iterative procedure to compute $\widehat{\mathbf{F}}^{(k)}$. Finally, to completely implement the IRLS algorithm, it remains to define the initial solution of each nested IRLS procedure as well as stopping criteria for both nested and outer loops.

The initial solution of the IRLS algorithm at outer iteration $k > 1$ is chosen as the solution of the following weighted Tikhonov regularization [25, 34]:

$$\begin{aligned} \widehat{\mathbf{F}}^{(k,0)} &= \underset{\mathbf{F}}{\operatorname{argmin}} \; \|\mathbf{X} - \mathbf{H}\mathbf{F}\|_2^2 + \alpha^{(k-1)} \left\| \mathbf{W}^{(k-1)^{1/2}} \left(\mathbf{F} - \widehat{\mathbf{F}}^{(k-1)} \right) \right\|_2^2 \\ &= \left[\mathbf{H}^H \mathbf{H} + \alpha^{(k-1)} \, \mathbf{W}^{(k-1)} \right]^{-1} \left[\mathbf{H}^H \mathbf{X} + \alpha^{(k-1)} \, \mathbf{W}^{(k-1)} \, \widehat{\mathbf{F}}^{(k-1)} \right]. \end{aligned} \tag{9}$$

For the particular case $k = 1$, the initial solution is computed from the previous relation using $\mathbf{W}^{(0)} = \mathbf{I}$ ($\mathbf{I}$: Identity matrix) and choosing $\alpha^{(0)}$ from the heuristic selection procedure described in [34].

Regarding now, the definition of the stopping criteria, it should be noted that the proposed non-stationary regularization offers a natural definition of the stopping criteria based on the relative variation of the adaptive regularization parameter between two successive outer or inner iterations. Formally,

the relative variations δ and γ of the adaptive regularization parameter for the inner and outer loops are respectively defined such that:

$$\delta = \frac{\left|\alpha^{(k,j)} - \alpha^{(k,j-1)}\right|}{\alpha^{(k,j-1)}} \quad \text{and} \quad \gamma = \frac{\left|\alpha^{(k)} - \alpha^{(k-1)}\right|}{\alpha^{(k-1)}}. \tag{10}$$

As classically done in the literature, the iterative processes are stopped when the relative variations δ and γ are less than or equal to some tolerance. Experimentally, it has been found that setting the tolerances to 10^{-8} and 10^{-2} for the inner and outer loops respectively allows obtaining consistent reconstructions, while preserving the computational performances of the overall resolution process.

3.2. Stationary version

The stationary iterated multiplicative regularization is directly derived from the non-stationary version by fixing once for all the values of the weighting matrix $\mathbf{W}^{(k)}$ and the adaptive regularization parameter $\alpha^{(k)}$ to their values obtained after the first main iteration (i.e. $k = 1$) of the non-stationary algorithm, that is:

$$\mathbf{W}^{(k)} = \overline{\mathbf{W}} := \mathbf{W}^{(1,N_j)} \quad \text{and} \quad \alpha^{(k)} = \overline{\alpha} := \alpha^{(1,N_j)}. \tag{11}$$

In other words, the stationary multiplicative regularization (SIMR) can be expressed as:

$$\begin{cases} \widehat{\mathbf{F}}^{(0)} = \mathbf{0} \\ \left(\widehat{\mathbf{F}}^{(1)}, \overline{\mathbf{W}}, \overline{\alpha}\right) = \underset{\mathbf{F}\setminus\{\mathbf{0}\}}{\operatorname{argmin}} \ \|\mathbf{X} - \mathbf{H}\mathbf{F}\|_2^2 \cdot \|\mathbf{F}\|_q^q & \text{for } k = 1 \\ \widehat{\mathbf{F}}^{(k)} = \underset{\mathbf{F}}{\operatorname{argmin}} \ \|\mathbf{X} - \mathbf{H}\mathbf{F}\|_2^2 + \overline{\alpha} \left\| \overline{\mathbf{W}}^{1/2} \left(\mathbf{F} - \widehat{\mathbf{F}}^{(k-1)}\right) \right\|_2^2 & \text{for } k \geq 2 \end{cases}. \tag{12}$$

At this stage, it is important to note that from $k = 2$, the explicit expression of the force vector $\widehat{\mathbf{F}}^{(k)}$ is:

$$\widehat{\mathbf{F}}^{(k)} = \left[\mathbf{H}^H\mathbf{H} + \overline{\alpha}\,\overline{\mathbf{W}}\right]^{-1}\left[\mathbf{H}^H\mathbf{X} + \overline{\alpha}\,\overline{\mathbf{W}}\,\widehat{\mathbf{F}}^{(k-1)}\right], \quad \text{for } k \geq 2. \tag{13}$$

Consequently, only the matrix $\mathbf{A} = \mathbf{H}^H\mathbf{H} + \overline{\alpha}\,\overline{\mathbf{W}}$ has to be inverted to compute $\widehat{\mathbf{F}}^{(k)}$ for any $k \geq 2$. This allows deriving a computationally efficient algorithm, since if $\mathbf{A}$ is factorized using a LU decomposition for instance, the overall computation of $\widehat{\mathbf{F}}^{(k)}$ for $k \geq 2$ is almost as expensive as than the computation of $\widehat{\mathbf{F}}^{(1)}$.

The main differences with the non-stationary version concerns the definition of the stopping criteria. As shown in Eq. 12, the proposed stationary iterated multiplicative regularization first requires the resolution of a multiplicative regularization at iteration $k = 1$ from the IRLS procedure described in Ref. [34], defining thoroughly the initial solution and the stopping criterion as in section 3.1. Here, the question is when to stop the main iteration loop. In the present case, because the adaptive regularization parameter remains constant after the first outer iteration, the stopping criterion is consequently related to the relative variation of the functional:

$$J(\widehat{\mathbf{F}}^{(k)}) = \|\mathbf{X} - \mathbf{H}\widehat{\mathbf{F}}^{(k)}\|_2^2 + \overline{\alpha}\,\left\|\overline{\mathbf{W}}^{1/2}\left(\widehat{\mathbf{F}}^{(k)} - \widehat{\mathbf{F}}^{(k-1)}\right)\right\|_2^2 \tag{14}$$

between two successive iterations. Practically, the algorithm is automatically stopped when a prescribed tolerance defined by the user is reached. Here, the tolerance is set to 10^{-2} as for the non-stationary version.

4. Numerical validation

This numerical validation intends to investigate the differences between the two proposed iterated multiplicative regularizations through two frequency-domain applications. In the present numerical validations, only the reconstruction of the spatial distributions of sources associated to a harmonic point force exciting the studied structures at a particular frequency is considered. This is not a limitation of the method, since the force spectrum or history can be reconstructed from the proposed approach provided that the system matrix $\mathbf{H}$ is established accordingly. Finally, it is also worth noting that all the reconstructions are performed outside resonance frequencies. Indeed, at resonance frequencies, the inverse problem is known to be difficult. Because the system matrix is singular, the uniqueness of the solution is not ensured and the identified solution is generally not satisfying whatever the regularization approach used. It follows that the corresponding refined solution is generally not satisfying at resonance frequencies as well.

4.1. 1D structure

In the present application, the studied structure is a free-free steel beam with dimensions $1\times0.03\times0.01$ m^3 excited by a unit point force at 350 Hz. The coordinate of the point force, measured from the left end of the beam, is $x_0 = 0.6$ m.

4.1.1. Synthesis of the vibration field

In this example, the reconstruction is performed from the displacement field $\mathbf{X}$ measured at 350 Hz over the structure. To synthesize the measured vibration field, two numerical steps have been implemented. First, a finite

element model of the beam made up with 20 plane beam elements has been used to compute the exact displacement field. Then, a Gaussian white noise with a prescribed SNR has been added to the exact data to simulate measurement errors, related to the transducers quality.

4.1.2. Reconstruction model

Let consider the practical situation where the vibration field $\mathbf{X}$, measured over the surface of a structure, is caused by an unknown excitation field $\mathbf{F}$. If the structure is linear, its dynamic behavior is completely determined by the transfer functions matrix $\mathbf{H}$, relating the vibration field $\mathbf{X}$ to the unknown field $\mathbf{F}$ by the relation:

$$\mathbf{X} = \mathbf{HF}. \tag{15}$$

In the present application, the FE model of the structure, used to compute the vibration field, has also been employed to compute the transfer functions matrix $\mathbf{H}$ by assuming that only bending motions are measurable. In other words, the transfer functions matrix have been dynamically condensed over the measurable dofs.

4.1.3. Application

To assess the validity of the proposed iterated multiplicative regularization strategy, it is compared to the ordinary multiplicative regularization (OMR). For this purpose, the choice of the tuning parameter q is crucial. The analysis of the numerical test case shows that the beam is only excited by a point force. In this context, it is reasonable to set $q = 0.5$.

In section 2, it has been shown that, for this application example, the excitation field identified from OMR was in line with the target one, when the reconstruction is based on measured data with a high SNR value (30 dB in the present case). Consequently, both versions of the iterated multiplicative regularization are expected to provide reconstructions similar to that obtained with OMR. To confirm this intuition quantitatively, the relative error of the reconstructed solution is evaluated for each regularization strategy and given in Table 1. Formally, the relative error is given by:

$$E = \frac{\|\mathbf{F_{ref}} - \mathbf{F_{id}}\|_2^2}{\|\mathbf{F_{ref}}\|_2^2}, \tag{16}$$

where $\mathbf{F_{ref}}$ is the reference excitation field and $\mathbf{F_{id}}$ is the force identified by OMR, NSMIR or SMIR. Furthermore, the computation time of each regularization strategy is also given in Table 1 to fairly compare their computational efficiency.

The results presented in Fig. 3 and Table 1 confirm our intuition, since the three approaches give similar reconstructions. It should however be noted that SMIR leads to a slightly better reconstruction for a computation time comparable to OMR, while NSMIR provides the same result as OMR for a computation time almost 30 times larger.

Perhaps more interestingly, for measured data with a low SNR level, the differences between each approach appear more clearly [see Fig. 4 and Table 2]. Indeed, when the reconstruction is performed from measured data having a SNR equal to 13 dB, only SMIR allows obtaining a far more better estimation of the point force amplitude than OMR, while preserving the overall quality of the reconstructed excitation field and the expected com-

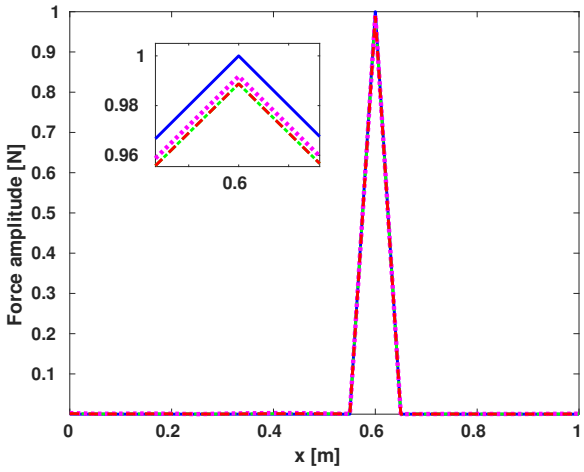

Figure 3: Spatial reconstruction of the excitation field at 350 Hz from a vibration field corrupted by an additive Gaussian white noise with a SNR of 30 dB - (—) Reference, (– –) OMR for $q = 0.5$, (– · –) NSIMR for $q = 0.5$ and (· · ·) SMIR for $q = 0.5$

Table 1: Relative error and computation times for OMR, NSMIR and SMIR obtained from a reconstruction performed at 350 Hz from a vibration field corrupted by an additive Gaussian white noise with a SNR of 30 dB for a 1D structure

Strategy	**Relative error** (%)	**Computation time** (ms)
OMR	0.013	8
NSMIR	0.013	218.5
SMIR	0.010	11.2

putational efficiency of the approach. In this case too, NSMIR gives the same reconstructed excitation field as OMR for a computation time much greater than OMR or SMIR. Actually, this potentially surprising result is related to the evolution of the value of the adaptive regularization parameter α of NSIMR over the main iterations. Indeed, it is of the order of 10^{13} from $k = 2$ until convergence of the resolution algorithm. In other words, this means that one necessarily has $\widehat{\mathbf{F}}^{(k)} \approx \widehat{\mathbf{F}}^{(k-1)}$ at each outer iteration. This result can be explained by the fact that, in NSIMR, the regularization parameter is optimally adapted in order to find a solution minimizing the residual solution $\mathbf{F} - \widehat{\mathbf{F}}^{(k-1)}$, which is not the case for SMIR. In addition, to have a global overview of the influence of the noise level on the solutions reconstructed from OMR and SMIR, a discussion is proposed in Appendix A. As a side note, it should however be noted that, below 10 dB, OMR (and so NSMIR and SMIR) fails in providing consistent solutions as highlighted by the various simulations we have run[2].

[2]This is not the case of the related additive regularization described in Ref. [25, 34] which is based on automatic a posteriori selection procedures like the L-curve to determine the associated regularization parameter λ. Consequently, if needed, one can implement a stationary iterated additive regularization by simply computing at $k = 1$ the solution of the related additive regularization and replacing from $k = 2$ the adapted regularization parameter $\bar{\alpha}$ by the regularization parameter $\bar{\lambda}$ obtained after the first outer iteration. The latter iterated regularization is however computationally more expensive than that proposed in this paper [34].

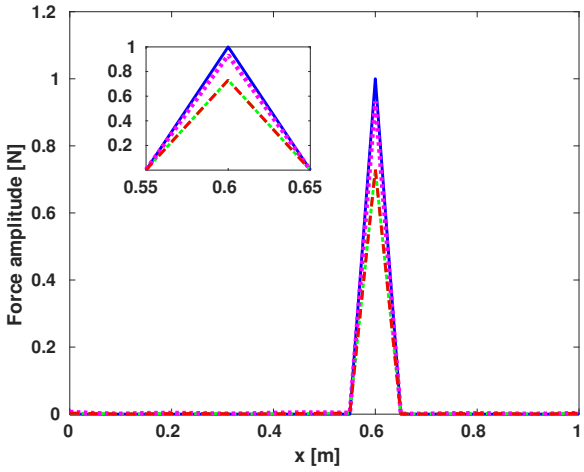

Figure 4: Spatial reconstruction of the excitation field at 350 Hz from a vibration field corrupted by an additive Gaussian white noise with a SNR of 13 dB - (—) Reference, (−−) OMR for $q = 0.5$, (− · −) NSIMR for $q = 0.5$ and (· · ·) SMIR for $q = 0.5$

Table 2: Relative error and computation times for OMR, NSMIR and SMIR obtained from a reconstruction performed at 350 Hz from a vibration field corrupted by an additive Gaussian white noise with a SNR of 13 dB for a 1D structure

Strategy	**Relative error** (%)	**Computation time** (ms)
OMR	7.28	42.6
NSMIR	7.28	167.7
SMIR	0.47	44.5

4.2. 2D structure

In this second application, the studied structure is a free-free steel plate with dimensions $0.6 \times 0.4 \times 0.005$ m^3. The coordinates of the point force, measured from the lower left corner of the plate, are $(x_0, y_0) = (0.247$ m, 0.218 m).

4.2.1. Synthesis of the vibration field

In this example, the reconstruction is performed from the velocity field $\mathbf{X}$ measured at 350 Hz over the structure. To properly simulate experimental measurements, the exact vibration displacement field $\mathbf{X_{exact}}$ is first computed from a FE mesh of the plate made up with 187 shell elements, assuming that only bending motions are measurable. Then, a Gaussian white noise with a prescribed SNR is added to the exact data to simulate measurement errors. In the next of this application, the generated exact data are corrupted so that the corresponding SNR is either equal to 30 dB or 13 dB.

4.2.2. Reconstruction model

As in section 4.1, the structure being linear, its dynamic behavior is governed by the transfer functions matrix $\mathbf{H}$, relating the vibration field $\mathbf{X}$ to the unknown field $\mathbf{F}$ through Eq. 15. The FE model of the structure, used to compute the vibration field, has also been employed to compute the transfer functions matrix $\mathbf{H}$ by assuming that only normal velocities are measurable. In other words, the transfer functions matrix have been dynamically condensed over the measurable dofs.

4.2.3. Application

The analysis of the test case suggests that the target excitation field is very sparse. Consequently, it is reasonable to set $q = 0.5$. In doing so, all the necessary ingredients are available for reconstructing the excitation field at 350 Hz from OMR, NSIMR and SMIR.

As shown in Figs. 5 and 6, all the regularization strategies gives excellent reconstructed excitation fields when the SNR is relatively high. Here again and for the same reasons as those pointed out in section 4.1, it is observed that OMR and NSMIR lead to the same reconstructed excitation field. Actually, the main differences are related to the computation time associated to each regularization strategy. Indeed, Table 3 shows that the computation time for OMR and SMIR are comparable, while that obtained for NSMIR is about 30 times larger.

Table 3: Relative error and computation times for OMR, NSMIR and SMIR obtained from a reconstruction performed at 350 Hz from a vibration field corrupted by an additive Gaussian white noise with a SNR of 30 dB for a 2D structure

Strategy	**Relative error** (%)	**Computation time** (ms)
OMR	0.028	45.6
NSMIR	0.028	1629.3
SMIR	0.016	50.9

Here again, the situation is rather different in case of low SNR, since SMIR exhibits higher performances than OMR/NSMIR, regarding the re-

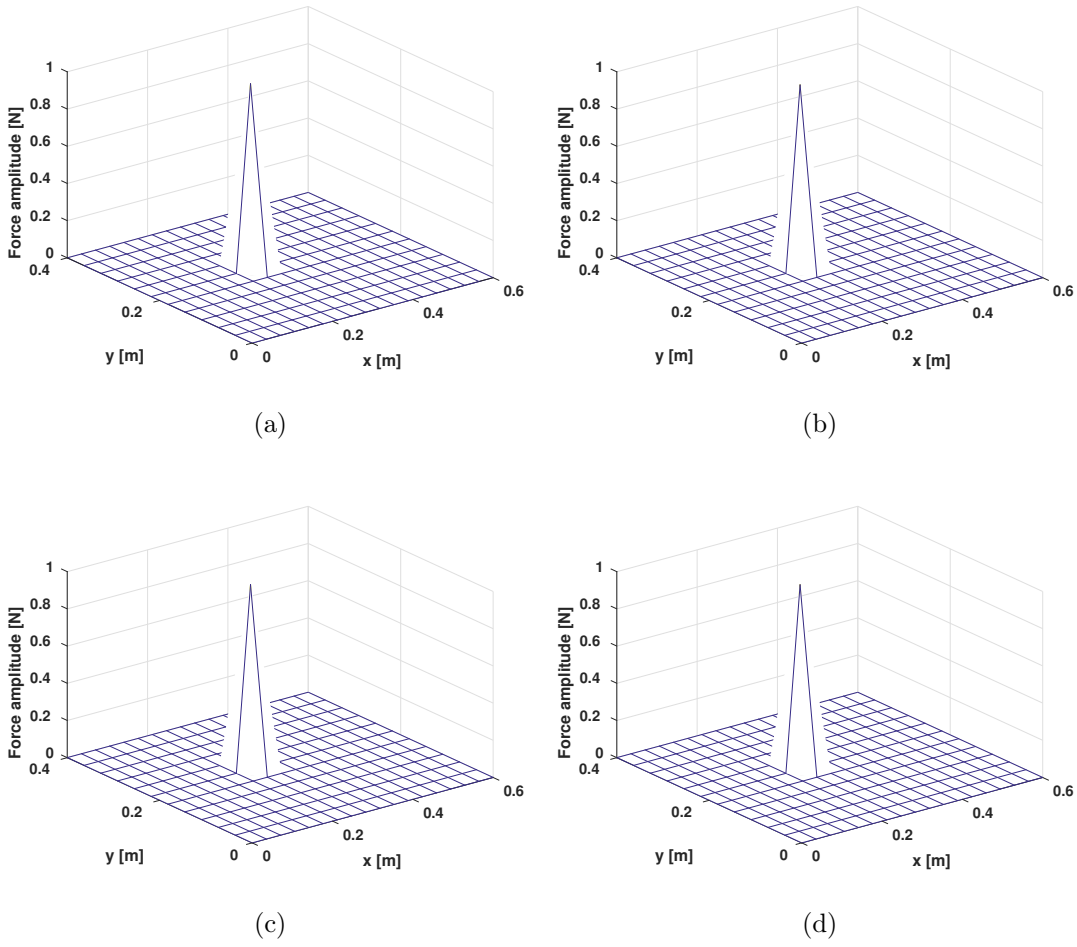

Figure 5: Reconstructed excitation field at 350 Hz for SNR = 30 dB - (a) Reference, (b) OMR, (c) NSMIR and (d) SMIR

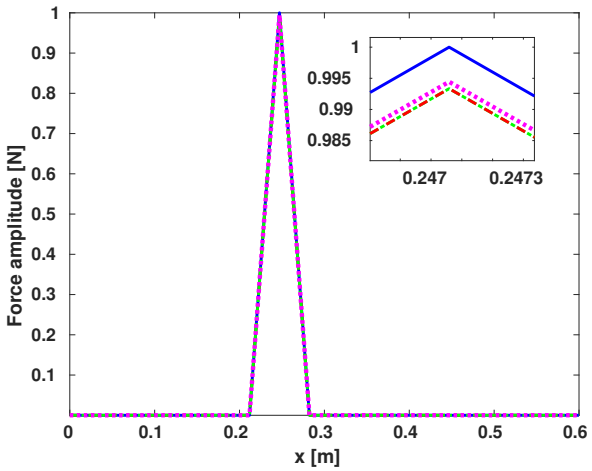

Figure 6: Section view of the reconstructed excitation field at $\widehat{y}_0 = 0.218$ m for SNR = 30 dB - (—) Reference, (– –) OMR for $q = 0.5$, (– · –) NSIMR for $q = 0.5$ and (· · ·) SMIR for $q = 0.5$

construction of the point force amplitude, since an improvement of 9% is obtained [see Figs.7 and 8 and Table 4]. Consequently, the application to a higher dimensional case confirms the observations made for the 1D case.

5. Experimental validation

The numerical validation has allowed drawing several interesting conclusions regarding the behavior of NSMIR and SMIR. First, NSMIR provides reconstructions similar to OMR. Second, SMIR significantly improves the quality of identified solutions in case of low SNR. To confirm all these conclusions, the analysis is extended to a real-world application, already used in Ref. [34] for validating OMR.

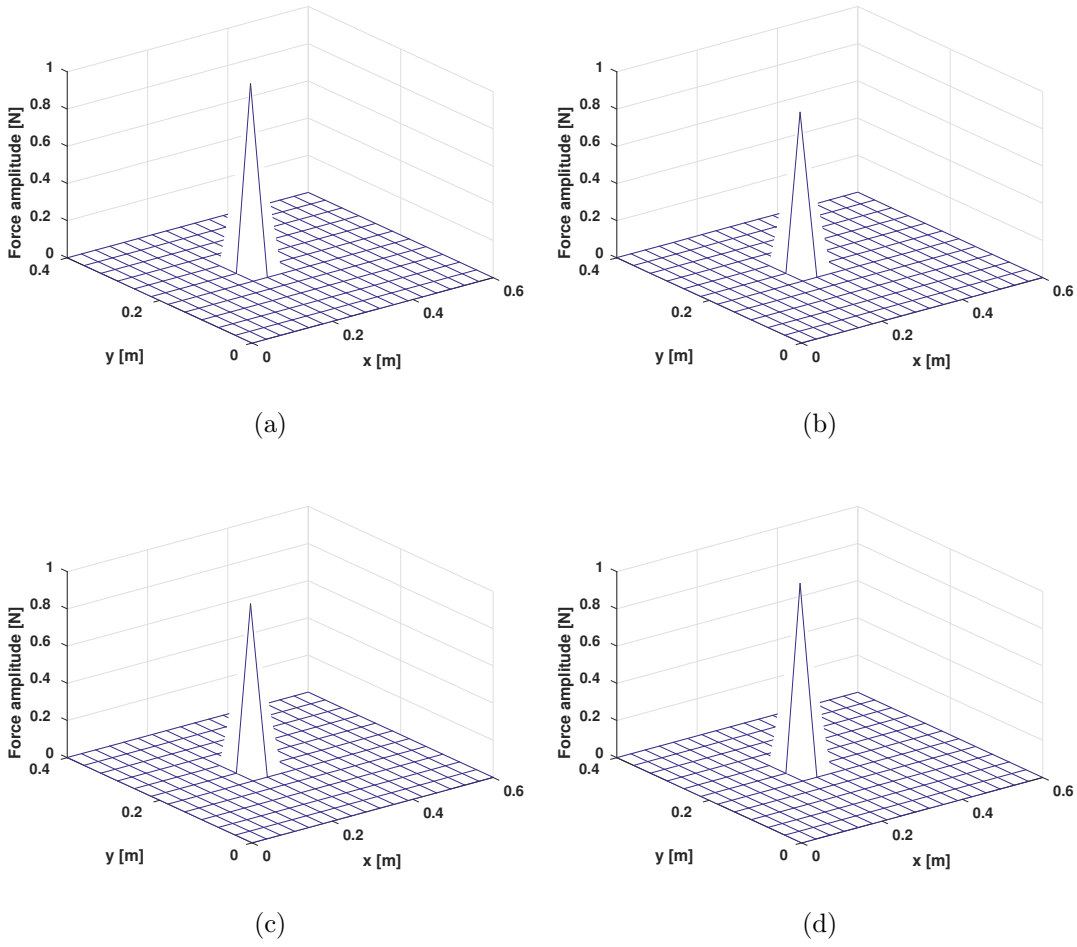

Figure 7: Reconstructed excitation field at 350 Hz for SNR = 13 dB - (a) Reference, (b) OMR, (c) NSMIR and (d) SMIR

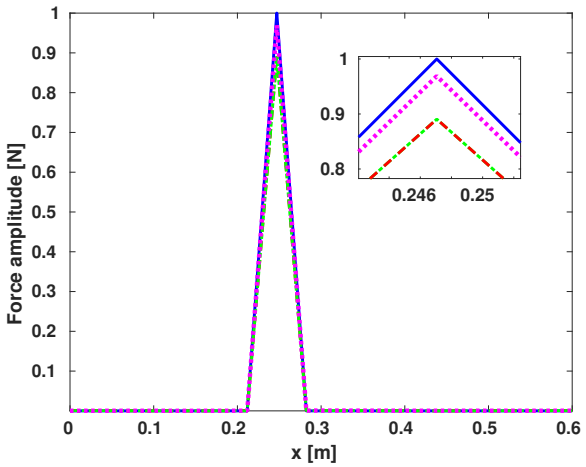

Figure 8: Section view of the reconstructed excitation field at $\widehat{y}_0 = 0.218$ m for SNR = 13 dB - (—) Reference, (– –) OMR for $q = 0.5$, (– · –) NSIMR for $q = 0.5$ and (· · ·) SMIR for $q = 0.5$

Table 4: Relative error and computation times for OMR, NSMIR and SMIR obtained from a reconstruction performed at 350 Hz from a vibration field corrupted by an additive Gaussian white noise with a SNR of 13 dB for a 2D structure

Strategy	**Relative error** (%)	**Computation time** (ms)
OMR	1.559	78.4
NSMIR	1.559	3125.9
SMIR	0.168	85.1

5.1. Description of the experimental set-up

The considered structure is a suspended (free) aluminum plate of 0.6 m in length, 0.4 m in width and 5 mm in thickness [see Fig. 9a]. The plate is excited at $(x_0, y_0) = (0.405 \text{ m}, 0.255 \text{ m})$ by a shaker fed by a white noise signal and equipped with a force sensor [see Fig. 9b].

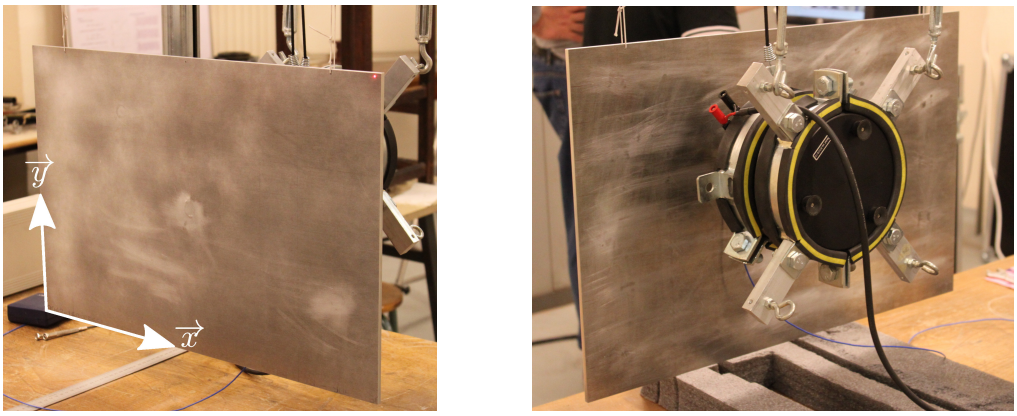

(a) (b)

Figure 9: Experimental set-up - (a) Suspended plate and (b) Excitation device

Measurements of the vibration field were carried out with a scanning laser vibrometer on a grid of 35×29 points along x and y directions respectively using the force signal as phase reference. Regarding the reconstruction model, the structure under test being linear, it can be expressed as in Eq. (15). In the present application, the transfer function matrix $\mathbf{H}$ has been computed from a FE mesh designed to perfectly match the measurement mesh. As a result, it is composed of 952 shell elements, making the model theoretically valid up to 4500 Hz. Moreover, the calculation has been performed, considering that

the bending motions as the only available data. In other words, the transfer functions matrix has been dynamically condensed over the measurable dofs. Finally, it is worth noting that a global structural damping is used in the present experimental validation. Its value has been estimated from the modal damping ratios obtained from the measured FRFs.

5.1.1. Application

Before applying the different regularization strategies, the norm parameter q must be determined beforehand. The analysis of the experimental set-up suggests that the target excitation field is very sparse. Consequently, it is reasonable to set $q = 0.5$.

In the present experimental validation, the reconstruction is performed at 300 Hz, i.e. outside resonance frequencies. As shown in Fig. 10, the reconstructed excitation fields from OMR, NSMIR and SMIR are consistent with the target one, since the point force location is estimated at $(\widehat{x}_0, \widehat{y}_0) = (0.404 \text{ m}, 0.256 \text{ m})$. However, as observed in the numerical validation, SMIR allows obtaining a slightly better estimation of the point force amplitude for a computation time comparable to OMR, while NSMIR leads, here again, to a reconstruction similar to OMR, but for a larger computation time. In the present example, the improvement brought by SMIR is not spectacular, since the improvement is about 6% compared to OMR/NSMIR. However, this result is in line with our experience of laser vibrometry that allows obtaining rather clean measurements.

In the present experiment, SMIR provides only a slight improvement of

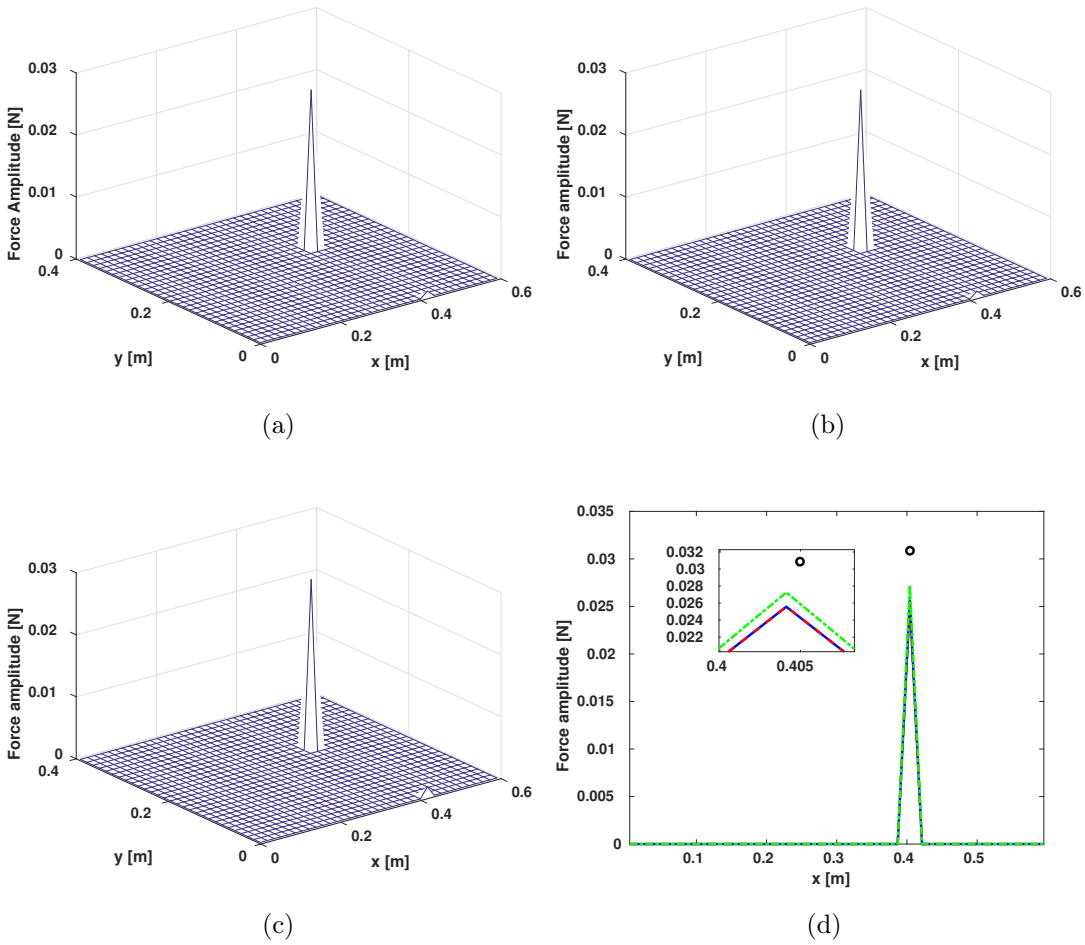

Figure 10: Amplitude of the reconstructed excitation field at 300 Hz - (a) Excitation field obtained from OMR, (b) Excitation field obtained from NSMIR, (c) Excitation field obtained from SMIR and (d) Section view at $\widehat{y}_0 = 0.256$ m - (—) OMR, (– –) NSMIR, (– · –) SMIR and (○) Location and amplitude of the measured force amplitude

Table 5: Computation times for OMR, NSMIR and SMIR obtained from a reconstruction performed at 300 Hz

Strategy	**Computation time** (s)
OMR	8.89
NSMIR	58.74
SMIR	14.16

the quality of the identified point force spectrum, since the results obtained from OMR are already in good agreement with the measured point force spectrum as demonstrated in Fig. 11 of Ref. [34].

6. Conclusion

In the present contribution, an original iterated multiplicative regularization has been presented for identifying mechanical sources acting on a structure. The underlying idea behind this regularization strategy was to combine the advantages of the iterated Tikhonov regularization, which can be thought as an iterative refinement of an initial solution obtained using the standard Tikhonov regularization, and the multiplicative regularization that eliminates the need for the selection of the regularization parameter while taking into account one's prior knowledge on the sources to identify. The resulting regularization strategy is aimed to be consequently flexible and computationally efficient. Practically, the iterated multiplicative regularization can be implemented in two different ways to give rise either to the non-stationary iterated multiplicative regularization (NSIMR) or to the stationary iterated multiplicative regularization (SIMR). Through numerical

and experimental validations, it has been shown that SIMR allows improving the quality of the reconstructed solutions, while NSMIR gives regularized solutions similar to that obtained from the ordinary multiplicative regularization. This surprising result has been documented and explained in the paper. However, the main conclusion of this paper is that SMIR can be used only when the measured data are very noisy (typically for SNR between 20 dB and 10 dB. In all other cases, the application of the ordinary multiplicative regularization is generally sufficient to obtain consistent reconstructions.

Appendix A. Influence of the noise level on the solutions identified from OMR and SMIR

This appendix aims at giving to the reader a better insight into the performances of the proposed iterated regularization strategy with respect to the noise level of the vibration data. To this end, reconstructions are performed on the application test case presented in section 4.1 from OMR and SMIR only for six different SNR (30 dB, 25 dB, 20 dB, 15 dB and 13 dB). As shown in Fig. A.11 and Table A.6, the quality of the solutions identified from OMR significantly deteriorates as the SNR decreases. This is surprisingly not the case when the reconstructions are performed from SMIR, for which the relative error increases much more slowly than for OMR. In the light of these results, it is reasonable to say that OMR can be used when the noise level is greater than 20 dB. Below 20 dB, it seems necessary to employ SMIR to expect obtaining a better solution accuracy.

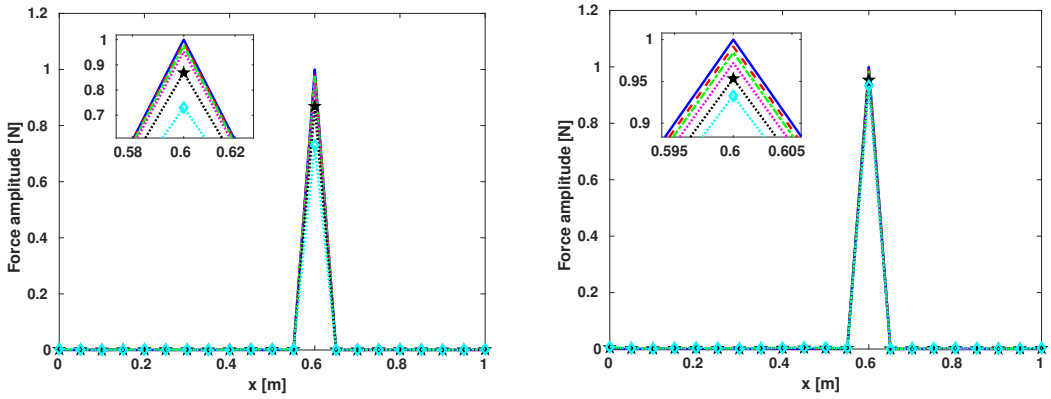

(a) (b)

Figure A.11: Spatial reconstruction of the excitation field at 350 Hz from a vibration field corrupted by an additive Gaussian white noise from (a) OMR and (b) SMIR – (—) Reference, (– –) SNR = 30 dB, (– · –) SNR = 25 dB, (· · ·) SNR = 20 dB, (· · ★ · ·) SNR = 15 dB and (· · ◇ · ·) SNR = 13 dB

Table A.6: Relative error (%) for OMR and SMIR for various noise levels

Strategy	**30 dB**	**25 dB**	**20 dB**	**15 dB**	**13 dB**
OMR	0.013	0.058	0.23	1.73	7.28
SMIR	0.010	0.035	0.08	0.23	0.47

References

[1] M. Hanke and C. W. Groetsch. Nonstationary iterated Tikhonove regularization. *Journal of Optimization theory and applications*, 98 (1):37–53, 1998.

[2] M. Donatelli. On nondecreasing sequences of regularization parameters for nonstationary iterated tikhonov. *Numerical Algorithms*, 60:651–668, 2012.

[3] M. Donatelli and M. Hanke. Fast nonstationary preconditioned iterative methods for ill-posed problems, with application to image deblurring. *Inverse Problems*, 29:095008 – 16pp, 2013.

[4] G. Huang, L. Reichel, and F. Yin. On the choice of solution subspace for nonstationary iterated tikhonov regularization. *Numerical Algorithms*, 72 (4):1043–1063, 2016.

[5] A. Buccini. Regularizing preconditioners by non-stationary iterated Tikhonov with general penalty term. *Applied Numerical Mathematics*, 116:64–81, 2017.

[6] A. Buccini, M. Donatelli, and L. Reichel. Iterated tikhonov regularization with a general penalty term. *Numerical Linear Algebra with Applications*, 24:e2089 – 12pp, 2017.

[7] J. T. King and D. Chillingworth. Approximation of generalized inverses by iterated regularization. *Numerical Functional Analysis and Optimization*, 1:5:499–513, 1979.

[8] H. W. Engl. On the choice of the Regularization Parameter for Iterated Tikhonov Regularization of Ill-Posed Problems. *Journal of Approximation Theory*, 49:55–63, 1987.

[9] H. Gfrerer. An a posteriori parameter choice for ordinary and iterated Tikhonov regularization of ill-posed problems leading to optimal convergence rates. *Mathematics of Computation*, 1987.

[10] O. Scherzer. Convergence rate of iterated tikhonov regularized solutions of nonlinear ill-posed problems. *Numerische Mathematik*, 66:259–279, 1993.

[11] Q.-N. Jin and Z.-Y. Hou. On the choice of the regularization parameter for ordinary and iterated regularization of nonlinear ill-posed problems. *Inverse Problems*, 13:815–827, 1997.

[12] A. N. Tikhonov. Regularization of incorrectly posed problems. *Soviet Mathematics*, 4:1624–1627, 1963.

[13] A. Cimetière, F. Delvare, M. Jaoua, and F. Pons. Solution of the cauchy problem using iterated tikhonov regularization. *Invers Problems*, 17:553–570, 2001.

[14] T. S. Jang and S. L. Han. Numerical experiments on determination of spatially concentrated time-varying load on a beam: an iterative regularization method. *Journal of Mechanical Science and Technology*, 23:2722–2729, 2009.

[15] Q. Jin and L. Stals. Nonstationary iterated Tikhonov regularization for

ill-posed problems in Banach spaces. *Inverse Problems*, 28:104011 – 15 pp, 2012.

[16] Q. Jin and M. Zhong. Nonstationary iterated Tikhonov regularization in Banach spaces with uniformly convex penalty terms. *Numerische Mathematik*, 127:485–513, 2014.

[17] F. Margotti and A. Rieder. An inexct Newton regularization in Banach spaces based on the nonstationary iterated Tikhonov method. *Journal of Inverse and Ill-Posed Problems*, 23 (4):373–392, 2015.

[18] S. Boyd and L. Vandenberghe. *Convex optimization*. Cambridge University Press, 2004.

[19] C. Renzi, C. Pezerat, and J.-L. Guyader. Vibratory source identification by using the finite element model of a subdomain of a flexural beam. *Journal of Sound and Vibration*, 332:545–562, 2013.

[20] R. Tibshirani. Regression shrinkage and selection via the lasso. *Journal of the Royal Statistical Society*, 58 (1):267–288, 1996.

[21] H. Fu, K. Ng, M. Nikolova, and J. L . Barlow. Efficient minimization methods of mixed $l_2 - l_1$ and $l_1 - l_1$ norms for image restoration. *SIAM Journal on Scientific Computing*, 27 (6):1881–1902, 2006.

[22] R. Chartrand and V. Stavena. Nonconvex regularization for image segmentation. In *Proccedings of International Conference on Image Processing, Computer Vision and Pattern Recognition (IPCV) 2007*, Las Vegas, USA, 2007.

[23] M. Grasmair. Non-convex sparse regularization. *Journal of Mathematical Analysis and Applications*, 365 (1):19–28, 2010.

[24] N. Chu, A. Mohammad-Djafari, and J. Picheral. Robust bayesian super-resolution approach via sparsity enforcing a priori for near-field aeroacoustic source imaging. *Journal of Sound and Vibrations*, 332 (18):4369–4389, 2013.

[25] M. Aucejo. Structural source identification using a generalized Tikhonov regularization. *Journal of Sound and Vibration*, 333(22):5693–5707, 2014.

[26] M. Aucejo and O. De Smet. Bayesian source identification using local priors. *Mechanical Systems and Signal Processing*, 66-67:120–136, 2016.

[27] B. Qiao, X. Zhang, J. Gao, R. Liu, and X. Chen. Sparse deconvolution for the large-scale ill-posed inverse problem of impact force reconstruction. *Mechanical Systems and Signal Processing*, 83:93–115, 2017.

[28] Q. Li and Q. Lu. A hierarchical bayesian method for vibration-based time domain force reconstruction problems. *Journal of Sound and Vibration*, 421:190–204, 2018.

[29] M. Aucejo and O. De Smet. On a full bayesian inference for force reconstruction problems. *Mechanical Systems and Signal Processing*, 104:36–59, 2018.

[30] P. C. Hansen. *Rank-Deficient and Discrete Ill-Posed Problems: Numerical Aspects of Linear Inversion*. SIAM, 1998.

[31] G. H. Golub, M. Heath, and G. Wahba. Generalized cross-validation as a method for choosing a good ridge parameter. *Technometrics*, 21 (2):215–223, 1979.

[32] A. Abubakar and P. M. van den Berg. Two - and three-dimensional algorithms for microwave imaging and inverse scattering. *Journal of Electromagnetic Waves and Applications*, 17:209–231, 2003.

[33] A. Abubakar, P. M. van den Berg, T. M. Habashy, and H. Braunish. A multiplicative regularization approach for deblurring problems. *IEEE Transactions on Image Processing*, 13:1524–1532, 2004.

[34] M. Aucejo and O. De Smet. A multiplicative regularization for force reconstruction. *Mechanical Systems and Signal Processing*, 85:730–745, 2017.

[35] M. Aucejo and O. De Smet. A space-frequency multiplicative regularization for force reconstruction problems. *Mechanical Systems and Signal Processing*, 104:1–18, 2018.

[36] M. Brill and E. Schock. Iterative solution of ill-posed problems: A survey. In *Model Optimization in Exploration Geophysics*, pages 13–38, Vieweg, Braunschweig, 1987.

[37] P. Rodriguez and B. Wohlberg. An iteratively weighted norm algorithm for total variation regularization. In *Proceedings of the 2006 Asilomar Conference on Signals, Systems, and Computers*, Pacific Grove, USA, 2006.